J Therm Anal Calorim (2012) 108:333–339
DOI 10.1007/s10973-011-1814-0

Thermal characterization of solid lipid nanoparticles containing praziquantel

Adelia Emilia de Almeida · Ana Luiza Ribeiro Souza · Douglas Lopes Cassimiro · Maria Palmira Daflon Gremião · Clóvis Augusto Ribeiro · Marisa Spirandeli Crespi

Received: 1 June 2011 / Accepted: 20 July 2011 / Published online: 4 August 2011

Abstract Solid lipid nanoparticles (SLNs), loaded and unloaded with praziquantel (PRZ-load SLN and PRZ-unload SLN) were prepared by two different procedures: (a) oil-in-water hot microemulsion method, obtaining at 70 °C an optically transparent blend composed of surfactant, co-surfactant, and water; and (b) oil-in-water microemulsion method, dissolving the lipid in an immiscible organic solvent, emulsified in water containing surfactants and co-surfactant, and then evaporated under reduced pressure at 50 °C. The mean diameter, polydispersity index (PdI), and zeta potential were 187 to 665 nm, 0.300 to 0.655, and −25 to −28 mV respectively, depending on the preparation method. The components, binary mixture, SLNs loaded and unloaded with PRZ, and physical mixture were evaluated by differential scanning calorimetry (DSC) and thermogravimetry (TG). The non-isothermal isoconversional Flynn-Wall–Ozawa method was used to determine the kinetic parameters associated with the thermal decomposition of the samples. The experimental data indicated a linear relationship between the apparent activation energy E and the pre-exponential factor A, also called the kinetic compensation effect (KCE), allowing us to determine the stability with respect to the preparation method. Loading with PRZ increased the thermal stability of the SLNs.

A. E. de Almeida (✉) · A. L. R. Souza · M. P. D. Gremião
Faculdade de Ciências Farmacêuticas, Departamento de Fármacos e Medicamentos, Universidade Estadual Paulista, Rodovia Araraquara-Jau Km 1 CP 502, Araraquara, SP 14801-902, Brazil
e-mail: almeidaa@fcfar.unesp.br

D. L. Cassimiro · C. A. Ribeiro · M. S. Crespi
Departamento de Química Analítica, Universidade Estadual Paulista, Instituto de Química, R. Prof. Francisco Degni, s/n, CP 355, Araraquara, SP 14801-970, Brazil

Keywords Solid lipid nanoparticles · SLN · Kinetic compensation effects · Praziquantel · Nonisothermal kinetics

Introduction

Schistosomiasis is a group of parasitic diseases caused by the species of trematodes, a helminths belonging to the genus *Schistosoma*. It is estimated that around two hundred million people are affected by schistosomiasis and that six hundred million people in the worldwide are exposed to the risk of contracting it [1]. Praziquantel (PRZ), 2 (*RS*)-2-(Cyclohexylcarbonyl) -1,2,3,6,7,11b-hexahydro-4*H*-pyrazino (2,1-alpha) isoquinolin-4-one (Fig. 1) is an effective anthelmintic against all the species of *Schistosoma,* and is the primary treatment for human schistosomiasis [2].

PRZ shows low solubility in water, about 400 mg/L, which translates into low bioavailability in the most commonly used pharmaceutical forms [3–5]. Therefore, technological alternatives to resolve the problem of drug release have been investigated. One promising strategy is the use ofSLNs as a releasing system to increase the bioavailability of lipophilic drugs [6–8].

SLNs have occupied a prominent position among the lipid systems for release of lipophilic drugs, by increasing their bioavailability and reducing pharmacokinetic variability. The term solid lipid nanoparticles (SLNs) was introduced in the 1990s [9, 10]. SLNs were developed as alternative carrier systems combining the advantages of polymeric nanoparticles (a controlled releasing solid matrix), the liposomes, and oil and water (O/W) emulsions. The use of SLN avoids the disadvantages of previous systems, such as instability resulting from the expulsion or coalescence of the drug, and improves the ease of

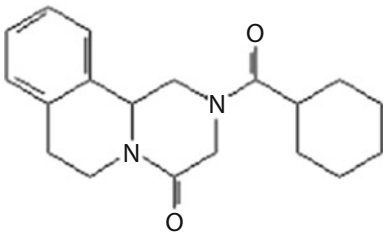

Fig. 1 Chemical structure of praziquantel (PRZ).

scheduling [11–19]. The SLN matrix is composed of lipids, which are solid at room and body temperatures, an emulsifying layer to stabilize the lipid dispersion, and water as the dispersion system, forming a mean particle size of 50–1,000 nm [20].

Kumar et al. [13] observed that the bioavailability of nitrendipine incorporated in SLN was increased 3–4 fold compared with the drug suspension. Luo et al. [21] prepared SLN containing vinpocetine, and through an oral pharmacokinetic study done on rats, they found that SLN significantly increased the bioavailability of the drug compared with the drug in solution.

The aim of this study is to prepare SLNs loaded with praziquantel by two different methods; to evaluate these preparations with respect to particle size, polydispersity index (PdI) and zeta potential (ZP), and to evaluate the interaction among the components forming SLN by DSC, the thermal stability by TG, and the kinetic parameters through the thermal decomposition step by the non-isothermal method.

Materials and methods

Materials

Praziquantel of pharmaceutical grade (min 99.8% provided by Shanghai Pharmaceuticals®) was used without further purification. Glyceryl monostearate (GMS lot 238), Sorbitan monostearate (SPAN 60 lot 0193), and Polyethyleneglycol sorbitan monostearate (TWEEN 60 lot 70HO912) were purchased from Henrifarma. Chloroform was provided by Merck.

Preparation of solid lipidic nanoparticles (SLN)

Preparation of SLN loaded with praziquantel by hot microemulsion method (PRZ-load SLN 75)

A mixture of GMS (0.2 g), Span 60 (0.1853 g), and PRZ (0.2 g) was heated at 75 °C, at a temperature above the melting point of GMS. TWEEN 60 (0.1147 g) was added to an aqueous phase (9.3 g) under stirring, heated to 75 °C, and added to the lipid phase. The obtained emulsion was sonicated at 120 W for 40 min in an ice bath. The product PRZ-load SLN 75 was then freeze-dried [21–23].

Preparation of SLN loaded with praziquantel by microemulsion and evaporation of the organic solvent (PRZ-load SLN 50)

A mixture of GMS (0.2 g), SPAN 60 (0.1853 g), and PRZ (0.2 g) was dissolved in chloroform (2.0 mL) and the organic solvent evaporated under reduced pressure and at a temperature of 50 °C. TWEEN 60 (0.1147 g) was added to an aqueous phase (9.3 g) under stirring, heated to 50 °C, and added to the lipid phase. The resulting emulsion was sonicated at 120 W for 40 min in an ice bath. The product PRZ-load SLN 50 was then freeze-dried [22, 24].

Preparation of binary mixture containing praziquantel (PRZ-GMS, PRZ-SPAN, PRZ-TWEEN), and physical mixture (MF)

The binary mixtures PRZ plus GMS, PRZ plus SPAN, and PRZ plus TWEEN were prepared by grinding the components in a mortar.

The physical mixture (MF) was prepared by grinding the components of SLN loaded with praziquantel in a mortar, without heating.

Thermal behavior

The TG curves were recorded in a TA Instruments SDT 2960 (simultaneous TG-DTA) using synthetic air atmosphere with flow rate of 130 mL min^{-1}, heating rate of 10 °C min^{-1}, and samples of 7.00 ± 0.5 mg. The curves were recorded from ambient temperature up to 600 °C.

DSC curves were obtained in a TA Instruments DSC 2920. Samples of 5.00 ± 0.25 mg were subjected to the thermal program (25–200 °C; 10 °C min^{-1} heating rate), in sealed 40 μL aluminum crucibles under a dynamic flow (50 mL min^{-1}) of N_2, in parallel with an empty crucible as reference.

Kinetic study

The mathematical description of the data from a single step solid-state decomposition is usually defined in terms of a kinetic triplet, with the activation energy (E), Arrhenius parameter (A), and a mathematical expression of the kinetic model as a function of the fractional conversion [f(α)], which can be related to the experimental data as follows [25]:

$$\frac{d\alpha}{dt} = A\exp\left(-\frac{E}{RT}\right)f(\alpha) \quad (1)$$

where T is temperature in degrees Kelvin, t is time in minutes, and α is the fractional conversion. For dynamic data obtained at a constant heating rate ($\beta = dT/dt$), this new term is inserted into Eq. 1, which can be simplified as

$$\frac{d\alpha}{dT} = \frac{A}{\beta}\exp\left(-\frac{E}{RT}\right)f(\alpha) \quad (2)$$

The activation energy from dynamic data can be obtained from the Flynn–Wall–Ozawa isoconversional method [26–28], with Doyle's approximation of $p(x)$. The $p(x)$ is defined by equation $\int_x^\infty e^{-x}/x^2 dx$, temperature integral or integral of Arrhenius [29] which involves the measurement of temperature corresponding to fixed values of $p(x)$ obtained from experiments at different β's and the plotting of $ln\ \beta$ versus $1/T$:

$$\ln\beta = \left[\frac{AE}{Rg(\alpha)}\right] - 5.331 - 1.052\frac{E}{RT} \quad (3)$$

where R is the universal gas constant (8.31432 K^{-1} J^{-1}) and $g(\alpha)$ is the integral of $d\alpha/f(\alpha)$ from 0 to α. This method allows one to obtain the apparent $E = E(\alpha)$ independently of the kinetic model, where $E(\alpha)$ is the activation energy for specific conversion degree (α). One evaluates the pre-exponential factor by taking into account that the reaction is a first-order one and can be defined as [30]:

$$A = \frac{\beta E}{RT_m^2}\exp\left(\frac{E}{RT_m}\right) \quad (4)$$

TG curves were recorded using nitrogen with a flow rate of 100 mL min^{-1} and at heating rates of 5, 10, and 20 °C min^{-1} and 2.00 ± 0.2 mg of sample. The curves were recorded from ambient temperature up to 400 °C. Only the decomposed fraction (α) from 0.05 to 0.95 was taken into account.

Determination of particle size, polydispersity (PdI), and zeta potential (ZP)

The size and polydispersity index of SLN in the dispersion were assessed by photon correlation spectroscopy (PCS) (Zetasizer Nano-ZS; Malvern Instruments, UK) at a fixed angle of 173° at 25 °C. The zeta potential was measured by laser Doppler anemometry using the same instrument at the same temperature. The samples were diluted with distilled water before analysis. Each value reported is the mean of the three measurements.

Results and discussion

The mean diameter, polydispersity index (PdI), and zeta potential were measured to characterize the SLNs, as shown in Table 1. The SLNs estimated by PCS had a size of 631.7 and 341.2 nm for PRZ-unloaded and PRZ-loaded SLN respectively, when prepared by the solvent-emulsification method (PRZ-load SLN 50). The SLNs prepared by hot microemulsion (PRZ-load SLN 75) showed a size of 187.3 and 364.8 nm for PRZ-unload and PRZ-load SLN, respectively. The size of all preparations was therefore in the desired colloidal range. Regarding the zeta potential, all the nanodispersions possessed a negative surface charge, suggesting that both praziquantel incorporation and the production method did not significantly change, the zeta potential of the SLNs. The loaded and unloaded nanoparticles showed an acceptable homogeneity in the size distribution, as indicated by the polydispersity index (PdI < 0.3).

Table 1 Mean particle sizes, PdI, and zeta potentials of the SLNs.

Formulations	Particle size/nm*	PdI	Zeta potential/mV
SLN 50	631.7 ± 74.0[a]	0.655 ± 0.100	−26.0 ± 1.0
PRZ-load SLN 50	341.2 ± 5.0[b]	0.412 ± 0.045	−26.7 ± 0.6
SLN 75	187.3 ± 1.7[c]	0.301 ± 0.052	−24.7 ± 1.2
PRZ-load SLN 75	364.8 ± 20.4[b]	0.485 ± 0.003	−27.6 ± 1.5

Means with the same letter are not significantly different

*Considered statistically significant for P-value < 0.05

The TG and DSC curves for PRZ, SLN-50, SLN-75, GMS, SPAN, TWEEN, binary mixture, MF and PRZ-load SLN 75, and PRZ-load SLN 50 are shown in Figs. 2 and 3, respectively, and the data obtained, from the curves are shown in Tables 2 and 3. Table 2, also includes DTA data from curves that are not shown here.

The majority of components were present in SLN melting before 70 °C, except for praziquantel (Fig. 3a–m, Table 3). The DSC curve for PRZ (Fig. 3d), showed a sharp pronounced endothermic peak, at 139.4 °C, assigned to the melting point of the drug [20].

The DSC curve (Fig. 3j) shows some interaction between GMS and PRZ characterized by changes in peak temperatures and its corresponding enthalpies. The GMS (Fig. 3a) shows an endothermic peak regarding the melting at 61.8 °C with enthalpy of 115.9 J/g; the binary mixture, PRZ-GMS, shows it at 65.2 °C and 56.9 J/g, respectively. The expected enthalpy in this case would be 57.9 J/g. In the region above 100 °C, the PRZ melting point decreased from 139.4 (Fig. 3d) to 106.7 °C (Fig. 3j). The observed enthalpy was 28.4 J/g, while the expected enthalpy would be 39.2 J/g.

The DSC curve (Fig. 3l) also showed some interaction between SPAN and PRZ. The binary mixture PRZ-SPAN, showed endothermic peaks at 65.3 and 104.9 °C having enthalpies of 31.9 and 24.5 J/g, respectively. The expected would be peaks at 55.7 and 139.4 °C with enthalpies

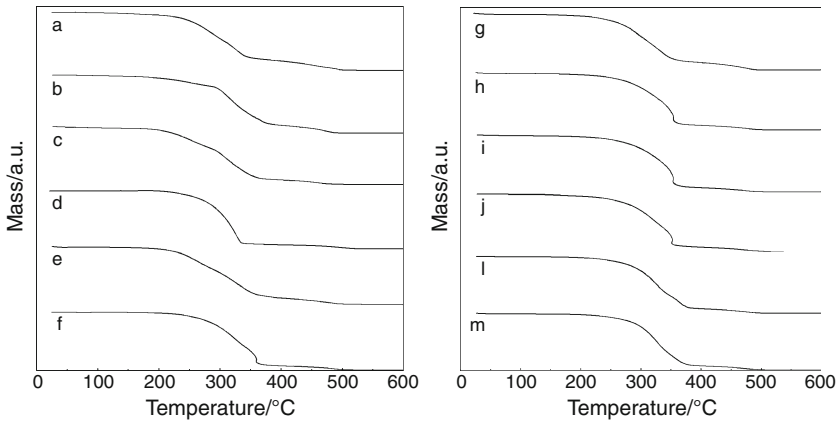

Fig. 2 TG curves for *a* GMS; *b* SPAN; *c* TWEEN; *d* PRZ; *e* SLN-50; *f* PRZ-load SLN 50; *g* SLN-75; *h* PRZ-load SLN 75; *i* MF; *j* PRZ-GMS; *l* PRZ-SPAN; *m* PRZ-TWEEN.

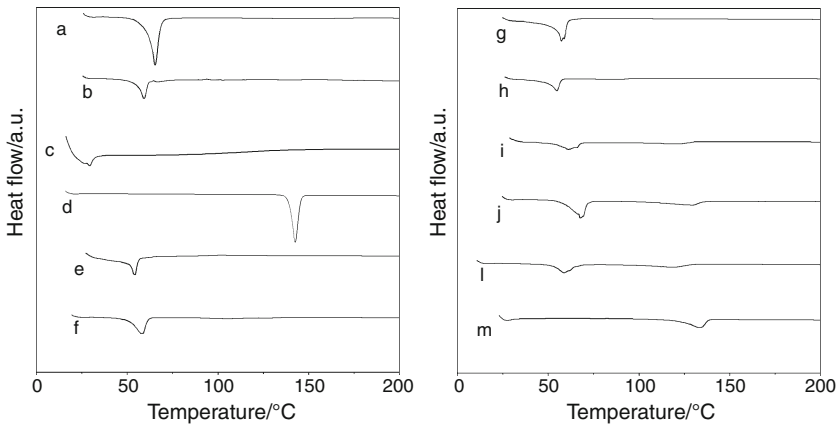

Fig. 3 DSC curves for: *a* GMS; *b* SPAN; *c* TWEEN; *d* PRZ; *e* SLN-50; *f* PRZ-load SLN 50; *g* SLN-75; *h* PRZ-load SLN 75; *i* MF; *j* PRZ-GMS; *l* PRZ-SPAN; *m* PRZ-TWEEN.

around 24.4 and 40.7 J/g, respectively. The smallest interaction was observed for the binary mixture between TWEEN and PRZ. The DSC curve showed the peak at 122.6 °C (39.3 J/g), and the expected peak would be 139.4 °C (39.2 J/g).

The DSC curve for the physical mixture (MF: Fig. 3i and Table 3) indicated the same behavior observed for the binary mixture PRZ-GMS and PRZ-SPAN, in which the presence of PRZ could still be observed. However, the most solubilization/interaction among the components was observed for the SLNs (Fig. 3e–h and Table 3). For the SLNs, only one endothermic peak between 50 and 60 °C was observed with enthalpy around 65–70 J/g except for PRZ –load SLN 50 for which it was 47.8 J/g. Therefore, both procedures to obtain the nanoparticles were efficient in promoting the interaction between lipid, surfactant, and PRZ.

The TG curves (Fig. 2a–m and Table 2) showed the thermal decomposition steps for individual, binary, and total components present inSLNs. The data for onset temperature indicated that the surfactants (TWEEN and SPAN) showed the lowest thermal stability regarding the lipid (GMS), which was lower compared with the loaded and unloaded SLNs. The highest thermal stability was observed for PRZ-unload SLN.

The PRZ-unload SLN (Fig. 2d) had its thermal decomposition point at 261.8 °C, while the nanoparticles PRZ–load SLN 50 (Fig. 2f) and PRZ–load SLN 75 (Fig. 2h) started in 255.9 *e* 253.9 °C, respectively. The unload nanoparticles, SLN-50 and SLN-75 (Fig. 2e, g), for which the thermal stability is around 223.9 and 253.1 °C respectively, showed some increase in thermal stability due to the presence of praziquantel (Table 2). However, considering only the temperature of the thermal decomposition steps, it is difficult to evaluate the real stabilization of the nanoparticles. Therefore, through the Flynn–Wall–Ozawa isoconversional method, considering the first thermal decomposition step, the apparent activation energies, E, at different conversional degrees, α, for the first thermal decomposition step and consequently the approximate pre-exponential factor could be obtained. Table 4 shows the mean values for E and lnA for PRZ, MF, SLN-50, SLN-75, PRZ- load SLN 75, and PRZ – load SLN 50.

There is a linear relationship between E and A, known as KCE (kinetic compensation effect), where a change in E corresponds to a change in A, expressed mathematically as $\ln A = a + bE$ (Fig. 4), suggesting the same mechanism for the thermal decomposition reaction for the samples to be evaluated. Therefore, the values for apparent activation

Table 2 Data for TG and DTA curves

Sample	Δm/%	ΔT/°C	T_{peak}/°C		T_{onset}/°C
			Endo	Exo	
GMS (a)	–	–	63		
	76.3%	100–351		331; 491	242
	21.1%	351–514			
SPAN (b)	–	–	55		
	20.3%	75–289			206
	63.7%	289–383		328; 350;366	
	15.2%	383–500		470	
TWEEN (c)	–	–	240		
	37.2%	97–291			213
	49.3%	291–372		332	
	9.6%	372–509		458	
PRZ (d)	–	–	140		
	90.1%	170–344		331	262
	9.1%	344–536		491	
SLN-50 (e)	–	–	50		
	81.1%	102–360		336	224
	16.6%	360–524		483	
PRZ–load SLN 50 (f)	–	–	56		
	64.9%	130–348			
	26.3%	348–370		359	256
	9.5%	370–535		486	
SLN-75 (g)	–	–	54		
	80.1%	54–362		335	253
	17.0%	362–509		465; 476	
PRZ–load SLN 75 (h)	–	–	51		
	87.1%	120–364	113	353	254
	10.9%	364–520		485	
MF (i)	–	–	59		
	86.9%	101–362		353	255
	11.0%	362–515		478	
PRZ-GMS (j)	–	–	64		
	57.5%	123–334		262	259
	32.3%	334–379		334	
	9.0%	379–550		454; 494	
PRZ-SPAN (l)	–	–	55		
	91.0%	160–412			277
	7.1%	412–543			455
PRZ-TWEEN (m)	–	–	130		
	457%	108–323			2689
	52.8%	323–546		369;471	

energy could be compared, indicating the following order for stability of the compounds, PRZ-load SLN 50 > MF > PRZ-load SLN 75 > PRZ > SLN-75 > SLN. This shows that SLN was stabilized by PRZ and that the preparation in organic solvent caused higher interactions among the components in PRZ – load SLN 50 than with hot microemulsion, as in PRZ – load SLN 75. Both nanoparticles obtained by microemulsion showed greater stabilization compared with unloaded SLN and PRZ, which is another advantage for this method of preparation.

Table 3 DSC curve data

Sample	T_{peak}/°C	T_{onset}/°C	ΔH/J/g
GMS (a)	62.3	61.8	115.9
SPAN (b)	59.2	55.4	50.8
TWEEN (c)	29.2	24.2	26.7
PRZ (d)	142.4	139.4	78.3
SLN-50 (e)	54.2	50.8	69.6
PRZ–load SLN 50 (f)	57.7	50.5	47.8
SLN 75 (g)	57.2	54.0	67.0
PRZ–load SLN 75 (h)	57.2	54.0	65.9
MF (i)	38.7–73.8	54.6	27.8
	97.1–135.3	105.8	12.6
PRZ-GMS (j)	67.6; 129.1	65.2; 106.7	56.9; 28.4
PRZ-SPAN (l)	58.7; 117.3	65.3; 104.9	31.9; 24.5
PRZ-TWEEN (m)	133.4	122.6	39.3

Table 4 Mean values for the activation energies (E) and pre-exponential factor ($\ln A$)

SAMPLES	ΔT/°C	$E \pm$ SD/kJ mol^{-1}	$\ln A \pm$ SD/min^{-1}
MF	240–350	88.00 ± 2.10	3.86 ± 0,11
PRZ	210–345	51.30 ± 11.10	0.42 ± 0.96
SLN -50	200–395	21.99 ± 2.00	2.55 ± 0.27
SLN -75	185–325	46.10 ± 16.60	0.03 ± 1.54
PRZ-load SLN 50	235–345	95.7 ± 24.00	4.52 ± 2.14
PRZ-load SLN 75	235–355	74.30 ± 10.00	2.59 ± 0.76

$X \pm$ SD (Mean ± standard deviation)

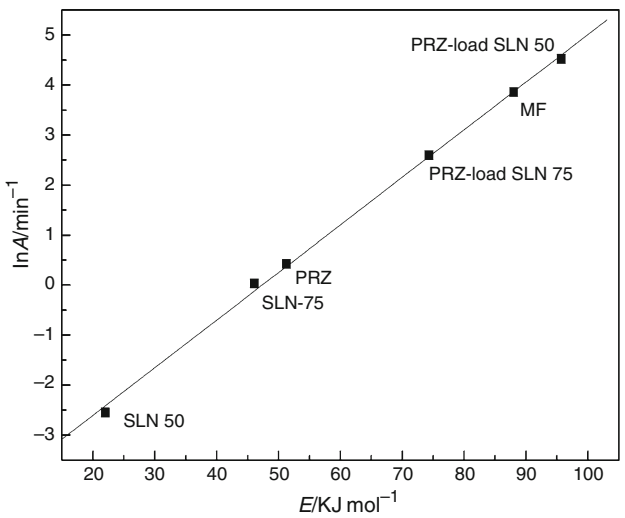

Fig. 4 Kinetic compensation effect for the first thermal decomposition of the samples.

Conclusions

Changes in the peak temperatures and enthalpy in the DSC curves of binary mixtures allowed us to identify a greater interaction among the drug (PRZ) with the lipid (GMS) and the surfactant (SPAN). Thus, the nanoparticles may show a distribution of PRZ between the lipid nuclei, GMS, and the layer surfactant layer, SPAN. This interaction was more effective in both methods, oil-in-hot water or in solvent microemulsion. The formation of the nanoparticles could be evaluated by the parameters of mean diameter, polydispersity index, and zeta potential. PRZ-loaded SLN showed a mean particle size of 350 nm with a narrow size distribution and high zeta potential value, indicating good physical stability.

The kinetic parameters of activation energy and pre-exponential factor could be obtained by the non-isothermal FWO method, and the kinetic compensation effect (KCE) observed for the set of samples allowed us to compare the thermal stability among the methods used to prepare the nanoparticles. The order of stability followed the sequence PRZ-load SLN 50 > MF > PRZ-load SLN 75 > PRZ > SLN-75 > SLN.

References

1. World Health Organization. Schistosomiasis. http://www.who.int/schistosomiasis/en. Accessed 22 Jan 2011.
2. Jeziorski MC, Greenberg RM. Voltage-gated calcium channel subunits from platyhelminths: potential role in praziquantel action. Int J Parasitol. 2006;36(6):625–32.
3. USP 31, NF 23. The United States Pharmacopeia and National Formulary. 2008;3056–7.
4. The Merck Index, Merck & Co. Inc., 13th ed. New York: Whitehouse Station; 2001.
5. Passerini N, Albertici B, Perissuti B, Rodriguez L. Evaluation of melt granulation and ultrasonic spray congealing as techniques to enhance the dissolution of praziquantel. Int J Pharm. 2006; 318(1–2):92–102.
6. Hu FQ, Zhang Y, Du YZ, Yuan H. Nimodipine loaded lipid nanospheres prepared by solvent diffusion method in a drug saturated aqueous system. Int J Pharm. 2008;348(1–2):146–52.
7. Müller RH, Runge SA, Ravelli V, Thünemann F, Mehnert W, Souto EB. Cyclosporine-loaded solid lipid nanoparticles (SLN®): Drug–lipid physicochemical interactions and characterization of drug incorporation. Eur J Pharm Biopharm. 2008;68(3):535–44.
8. Joshi M, Patravale V. Nanostructured lipid carrier (NLC) based gel of celecoxib. Int J Pharm. 2008;346(1–2):124–32.
9. Gasco MR. Method for producing solid lipid microspheres having a narrow size distribution. US Patent 1993;No. 5,250,236.
10. Müller RH, Lucks JS. Medication vehicles made of solid lipid particles (solid lipid nanospheres—SLN). European Patent 1996; No. 0605497.
11. Fricker G, Kromp T, Wendel A, Blume A, Zirkel J, Rebmann H, Setzer C, Quinkert RO, Martin F, Müller-Goymann C. Phospholipids and lipid-based formulations in oral drug delivery. Pharm Res. 2010;27:1469–86.

12. Kristl J, Volk B, Ahlin P, Gombac K, Sentjurc M. Interactions of solid lipid nanoparticles with membranes and leukocytes studied by EPR. Int J Pharm. 2003;256:133–40.
13. Kumar VV, Chandrasekar D, Ramakrishna S, Kishan V, Rao YM, Diwan PV. Development and evaluation of nitrendipine loaded solid lipid nanoparticles: influence of wax and glyceride lipids on plasma pharmacokinetics. Int J Pharm. 2007;335: 167–75.
14. Lin X, Li X, Zheng L, Yu L, Zhang Q, Liu W. Preparation and characterization of monocaprate nanostructured lipid carriers. Colloids and Surf A. 2007;311:106–11.
15. Muller RH, Mader K, Gohla S. Solid lipid nanoparticles (SLN) for controlled drug delivery - a review of the state of the art. Eur J Pharm Biopharm. 2000;50:161–77.
16. Radomska-Soukharev A. Stability of lipid excipient in solid lipid nanoparticles. Adv Drug Deliver Rev. 2007;59:411–8.
17. Westesen K, Bunjes H. Do nanoparticles prepared from lipids solid at room temperature always possess a solid lipid matrix? Int J Pharm. 1995;115:129–31.
18. Bunjes H, Unruh T. Characterization of lipid nanoparticles by differential scanning calorimetry, X-ray and neutron scattering. Adv Drug Deliver Rev. 2007;59:379–402.
19. Liu H, Li S, Wang Y, Yao H, Zhang Y. Effect of vehicles and enhancers on the topical delivery of cyclosporine A. Int J Pharm. 2006;311:182–6.
20. Mainardes RM, Chaud MV, Gremião MPD, Evangelista RC. Development of praziquantel-loaded PLGA nanoparticles and evaluation of intestinal permeation by the everted gut sac model. J Nanosci Nanotechnol. 2006;6:3057–61.
21. Luo Y, Chen D, Ren L, Zhao X, Qin J. Solid lipid nanoparticles for enhancing vinpocetine's oral bioavailability. J Control Release. 2006;114:53–9.
22. Mehnert W, Mader K. Solid lipid nanoparticles: production, characterization and applications. Adv Drug Deliver Rev. 2001; 47:165–96.
23. Pedersen N, Hansen S, Heydenreich AV, Kristensen HG, Poulsen HS. Solid lipid nanoparticles can effectively bind DNA streptavidin and biotinylated ligands. Eur J Pharm Biopharm. 2006; 62:155–62.
24. Mendoza AE, Companero MA, Mollinedo F, Blanco-Prieto MJ. Lipid nanomedicines for anticancer drug therapy. J Biomed Nanotechnol. 2009;5:323–43.
25. Brown ME, Dolimore D, Galwey AK. Reactions in the solid state: comprehensive chemical kinetics. Amsterdam: Elsevier; 1980.
26. Flynn JH, Wall LA. General treatment of the thermogravimetry of polymers. J Res Natl Bur Stand A. 1966;70:487–523.
27. Flynn JH, Wall J. A quick direct method for the determination of activation energy from thermogravimetric data. Polym Lett. 1966;4:323–8.
28. Dahiya JB, Kumar K, Muller-Hagedorn M, Bockhom H. Kinetics of isothermal and non-isothermal degradation of cellulose: model-based and model-free methods. Polym Int. 2008;57:722–9.
29. Doyle CD. Estimating isothermal life from thermogravimetric data. J Appl Polym Sci. 1962;6:639–42.
30. Kissinger HE. Reaction kinetics in differential thermal analysis. Anal Chem. 1957;29:1702–6.